Journal of
Mechanics of
Materials and Structures

MECHANICAL BEHAVIOR AND CONSTITUTIVE MODELING OF METAL CORES

Ashkan Vaziri and Zhenyu Xue

Volume 2, Nº 9 November 2007

mathematical sciences publishers

JOURNAL OF MECHANICS OF MATERIALS AND STRUCTURES
Vol. 2, No. 9, 2007

MECHANICAL BEHAVIOR AND CONSTITUTIVE MODELING OF METAL CORES

ASHKAN VAZIRI AND ZHENYU XUE

Studying the mechanical behavior of metal cores provides insight into the overall performance of structures comprising metal sandwich plates, and can help immensely in designing metal sandwich plates for specific engineering applications. In this study, the response of folded (corrugated) plate and pyramidal truss cores are explored under both quasistatic and dynamic loadings. In particular, two important characteristics of metal cores, the nonuniform hardening/softening evolution due to stressing in different directions and the rate-dependence, are discussed for different core topologies, including the square honeycomb core. In addition, the role of core behavior on the overall performance of sandwich plates is studied by employing a constitutive model for the elastic-plastic behavior of plastically compressible orthotropic materials [Xue et al. 2005]. The constitutive model is capable of capturing both the anisotropy of the core, associated with stressing in different directions, and its rate-dependence. The approach, based on employing the core constitutive model, not only significantly reduces the computation time, but also permits exploration of the role of each fundamental rate-dependent response of the metal core on the overall response of the metal sandwich plates.

1. Introduction

Recent studies have indicated the advantage of well-designed metal sandwich plates over solid plates under high intensity dynamic loading, where combinations of high strength and energy absorption are vital for the structural performance [Qiu et al. 2003; Xue and Hutchinson 2004a; Fleck and Deshpande 2004; Rathbun et al. 2006; Vaziri and Hutchinson 2007; Vaziri et al. 2007]. Metal sandwich plates encompass further advantages when the high intensity loading is transmitted through water, which can make them an excellent choice for ship protection [Xue and Hutchinson 2003; Hutchinson and Xue 2005; Liang et al. 2007]. On the other hand, sandwich plates with foam-filled cores have been shown to perform as well, or nearly as well, as plates of the same weight with unfilled cores [Vaziri et al. 2006]. Therefore, it appears that the multifunctional advantages of foam-filled cores such as acoustic and thermal insulation can be exploited without jeopardizing the structural performance of metal sandwich plates.

The volume fraction of the core occupied by metal and the core topology are important design aspects of all-metal sandwich plates [Xue and Hutchinson 2004a]. Three core topologies that have been commonly considered in the design of high-performance structures are square honeycomb, folded plate (corrugated) and pyramidal truss cores. Full-scale metal sandwich plates designed to be effective against impulsive loads have cores with a low volume fraction of material, typically less than 0.08 [Hutchinson

Keywords: constitutive modeling, plasticity, rate-dependence, sandwich plate, folded core, pyramidal truss core, finite element method.

This work has been supported in part by the ONR under grants GG10376-114934 and N00014-02-1-0700, and in part by the School of Engineering and Applied Sciences, Harvard University.

and Xue 2005]. In this study, the volume fraction of the core material is 2%, which is lower than the optimum configuration suggested by Xue and Hutchinson [2004a] for sandwich plates with the overall geometry in the meter scale. The rationale for studying thinner cores is based on their potential advantage for water blast by accounting for fluid-structure interaction [Liang et al. 2007]. Studying the behavior of metal cores not only provides insight regarding the overall performance of metal sandwich plates but also is required for developing a continuum model for sandwich plates. While the structural behavior of square honeycomb sandwich cores has been documented in recent numerical and theoretical investigation [Xue et al. 2005; Xue and Hutchinson 2006], the behavior of folded plate and pyramidal truss cores has not been studied rigorously. Consequently one of the main objectives of this study is to explore the mechanical response of folded and pyramidal truss cores under quasistatic and dynamic loadings (Sections 3 and 4). In Section 5, insight into the structural role of metal cores on the overall performance of sandwich plates is gained by employing a constitutive model proposed for the elastic-plastic behavior of plastically compressible orthotropic materials with nonuniform hardening or softening evolution associated with stressing in different directions [Xue et al. 2005]. In particular two intrinsic characteristics of the metal core, Nonuniform hardening/softening, and rate-dependence, are considered and their influence on the overall response of a folded sandwich plate is examined. The inputs to this constitutive model are identified based on the numerical simulation of the folded plate core behavior discussed in Section 3. All the calculations in this study are performed by employing the commercially available software ABAQUS [Abaqus 2005].

2. Specification of sandwich plates and material properties

Figure 1 shows the schematic diagram of folded plate and pyramidal truss core sandwich plates considered in this study. Both types of sandwich plates have core height H and face sheet thickness h. The folded plate core has thickness t and an inclination angle between the core web and the face sheet α, while the width of its periodic section is $B = t/\sin\alpha + H/\tan\alpha$. All members of the pyramidal truss core are identical and have solid square cross-sections of width t. Each truss member has three neighbors coming into contact at their corners with an angle of inclination between the truss and the face sheet, α. The width of a periodic section of the pyramidal truss core sandwich plate is $B = (t + t/\sin\alpha + H/\tan\alpha)/\sqrt{2}$.

For the *folded plate core*, the volume fraction of the core occupied by the material can be expressed as,

$$\bar{\rho}_c = \frac{t/H}{t/H + \cos\alpha}. \tag{1}$$

Similarly for the *pyramidal truss core,*

$$\bar{\rho}_c = \frac{2\sin\alpha}{(1 + \sin\alpha + \cos\alpha \cdot H/t)^2}, \tag{2}$$

and the total mass/area of the sandwich plate, M, is given by

$$M = \rho_s(2h + \bar{\rho}_c H). \tag{3}$$

For both types of sandwich plate, with L, M, and ρ_s specified, the geometry of the plate is fully determined by the three independent dimensionless parameters $\bar{\rho}_c$, H/L, and α. The face sheet thickness, h/L, is then determined in terms of $\bar{\rho}_c$ and H/L by Equation (3). Note that the top and bottom faces are

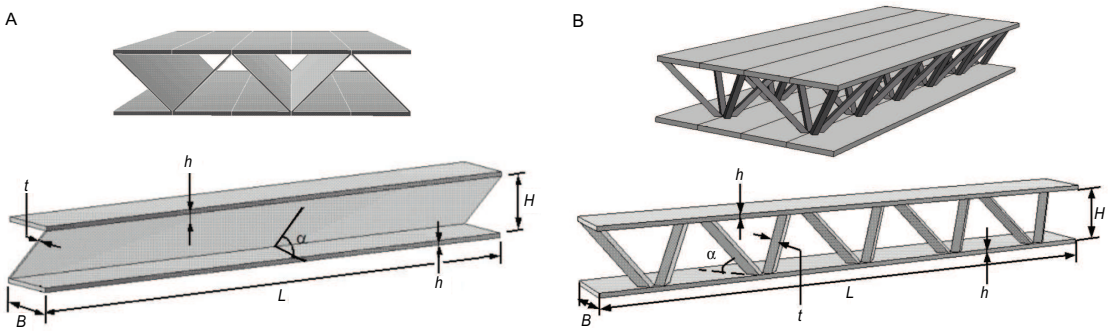

Figure 1. Schematic diagram of sandwich panels and corresponding computation model of sandwich panel: (a) folded sandwich plate; (b) pyramidal truss sandwich panel.

taken to have equal thickness in this study. In all the calculations presented in this paper, the following parameters are set to be constant: $M/\rho_s L = 0.02$, $H/L = 0.1$ and $L = 1$ m (width of the sandwich plates $= 2$ m).

The core and face sheets material of the sandwich plates are taken to be stainless steel (#304) with density of $\rho_s = 8000\,\text{kg/m}^3$. A piecewise function has been fitted to the true stress-logarithmic strain tensile behavior of the material, giving

$$\sigma = \begin{cases} E\varepsilon, & \varepsilon \le \sigma_Y/E, \\ \sigma_Y(E\varepsilon/\sigma_Y)^N, & \varepsilon > \sigma_Y/E, \end{cases} \tag{4}$$

with Young's modulus $E = 200$ GPa, Poisson ratio $\nu = 0.3$, tensile initial yield strength $\sigma_Y = 205$ MPa, and strain hardening exponent $N = 0.17$ [Boyer and Gall 1985]. The shear modulus and initial shear strength are $G = E/[2(1+\nu)] = 76.92$ GPa and $\tau_Y = \sigma_Y/\sqrt{3} = 118.35$ MPa. The material strain rate sensitivity of the steel is not taken into account. Classical flow theory of plasticity, based on the von Mises yield surface and isotropic hardening, is employed in the three-dimensional finite element simulations. The steel is assumed to be sufficiently ductile to sustain large strains without fracture.

3. Folded core unit cell response

The unit cell corresponding to the geometry of a folded plate core, along with the coordinate system used to define the anisotropy, are given in Figure 2a. Estimates of the overall elastic moduli associated with stressing in the directions of orthotropy, out-of-plane shearing, and in-plane shearing in two directions are obtained based on simple strength of materials formulas as described in [Xue and Hutchinson 2004b]:

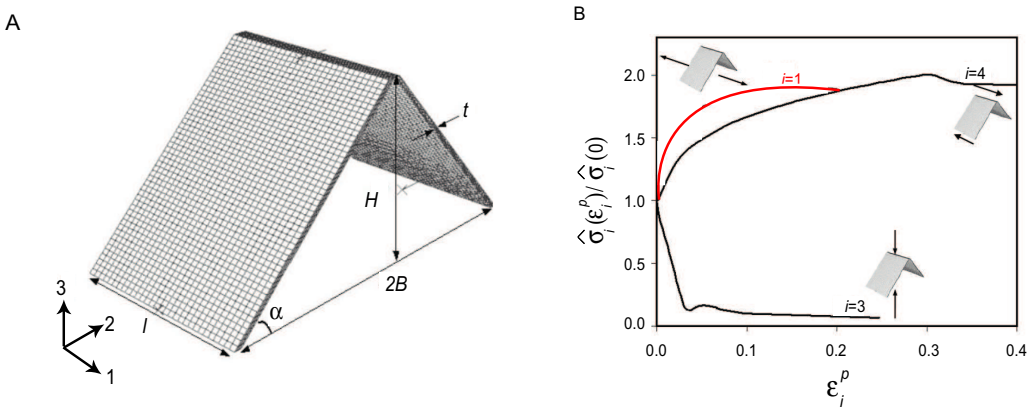

Figure 2. Mechanical behavior of folded plate cores: (a) finite element model of the folded core unit cell. (b) normalized true stress-true plastic strain relationships for three basic histories of the folded core with $\alpha = 45°$, $t/H = 0.0144$, corresponding to $B/H = 1.042$ and $\bar{\rho}_c = 0.02$. The true stresses are normalized by the theoretical values of the initial yield stress associated with each loading history under quasistatic loading, Equation (7). The horizontal axis is the plastic strain component ε_i^p associated with each stress history.

$$
\begin{aligned}
E_{11} &= \bar{\rho}_c E_s, \\
E_{33} &= \bar{\rho}_c E_s \sin^4 \alpha, \\
G_{13} &= \frac{1}{2} G_s \bar{\rho}_c \sin 2\alpha, \\
G_{23} &= \frac{1}{4} E_s \bar{\rho}_c \sin^2 2\alpha, \\
G_{12} &= \bar{\rho}_c G_s \sin^2 \alpha.
\end{aligned}
\tag{5}
$$

Let the x_i axes be aligned with the orthotropic axes. Introduce stress, strain, and plastic strain vectors in the usual way with

$$
\begin{aligned}
\boldsymbol{\sigma} &= (\sigma_1, \sigma_2, \sigma_3, \sigma_4, \sigma_5, \sigma_6)^T \equiv (\sigma_{11}, \sigma_{22}, \sigma_{33}, \sigma_{13}, \sigma_{23}, \sigma_{12})^T, \\
\boldsymbol{\varepsilon} &= (\varepsilon_1, \varepsilon_2, \varepsilon_3, \varepsilon_4, \varepsilon_5, \varepsilon_6)^T \equiv (\varepsilon_{11}, \varepsilon_{22}, \varepsilon_{33}, 2\varepsilon_{13}, 2\varepsilon_{23}, 2\varepsilon_{12})^T, \\
\boldsymbol{\varepsilon}^P &= (\varepsilon_1^P, \varepsilon_2^P, \varepsilon_3^P, \varepsilon_4^P, \varepsilon_5^P, \varepsilon_6^P)^T \equiv \left(\varepsilon_{11}^P, \varepsilon_{22}^P, \varepsilon_{33}^P, 2\varepsilon_{13}^P, 2\varepsilon_{23}^P, 2\varepsilon_{12}^P\right)^T.
\end{aligned}
\tag{6}
$$

Estimates for the initial quasistatic yield values in the directions of orthotropy, $\hat{\sigma}_i(0)$, are given by,

$$
\begin{aligned}
\hat{\sigma}_1(0) &= \bar{\rho}_c \sigma_Y, \\
\hat{\sigma}_3(0) &= \frac{2}{\sqrt{3}} \bar{\rho}_c \sigma_Y \sin^2 \alpha, \\
\hat{\sigma}_4(0) &= \hat{\sigma}_6(0) = \bar{\rho}_c \tau_Y \sin \alpha, \\
\hat{\sigma}_5(0) &= \frac{1}{2} \bar{\rho}_c \sigma_Y \sin 2\alpha.
\end{aligned}
\tag{7}
$$

As in the case of overall elastic stiffness, these estimates are based on elementary estimates from the strength of materials, and it was assumed that under crushing, yielding precedes the buckling of the core plate. The factor $(2/\sqrt{3})$ (for web materials having a von Mises yield surface) reflects the constraint of the faces such that the webs undergo plane strain tension (compression). It is noteworthy that E_{22} and $\hat{\sigma}_2(0)$ are exceedingly low and essentially irrelevant to the overall performance of sandwich plates as the faces supply essentially all the tensile strength and stiffness. In the calculations, they are taken as $\hat{\sigma}_2(0) = \bar{\rho}_c \sigma_Y/200$, and $E_{22} = \bar{\rho}_c E_s/200$.

The core responses under both quasistatic and dynamic loadings are calculated for a folded plate core having $\alpha = 45^\circ$ and $t/H = 0.0144$, (corresponding to $\bar{\rho}_c = 0.02$).

3.1. ***Numerical results for unit cell response under quasistatic loading.*** Periodic boundary conditions consistent with each loading history are imposed on the unit cell of the folded plate core. Under compression and shear loadings, rigid plates are bonded to top and bottom surfaces of the unit cell to simulate the behavior of the core attached to the face sheets. The bottom rigid plate is fixed and the top face is displaced. Figure 2b depicts the strain-stress curves of the folded plate core computed for three basic loading histories: in-plane stretching, out-of-plane shearing, and core crushing in the vertical direction. The dimensions of the folded core under study are such that under crushing, elastic buckling precedes yielding and the compression curve, $\hat{\sigma}_3(\varepsilon_3^P)$, falls sharply with buckling and yielding. Under out-of-plane shear, the response subsequent to buckling depends on the length of the segment as discussed in [Xue and Hutchinson 2004b]. In the results shown in Figure 2b, the length of the unit cell is taken to be equal to B, where yielding occurs prior to elastic buckling, and plastic buckling is the source of nonlinear deformation. Similar calculations were performed in [Xue and Hutchinson 2004b] and [Vaziri et al. 2006] for a higher relative density of the core, where yielding of the steel core precedes its elastic buckling under crushing. At early stages of deformation under out-of-plane shear ($\varepsilon_4^p < 0.2$), the shear-induced compaction of the core is almost zero, which corresponds to associated flow with respect to the ellipsoidal yield surface [Mohr et al. 2006].

In order to gain insight into the interaction among the stresses under multiaxial stressing, the initial yield surface of the folded core, defined as the onset of significant nonlinearity for the present purpose, is attained using the three-dimensional unit cell for two combinations of loading: (i) in-plane tension and core crushing (σ_1, σ_3), and (ii) core crushing and out-of-plane shear (σ_3, σ_4). The calculations are performed to simulate the response of the core unit cell under displacement control loading. Various ratios of displacements associated with each combined loading are imposed to specify the initial yield surface. The boundary conditions for the core under combined core crushing and out-of-plane shear are akin to the boundary conditions employed for calculating the strain-stress behavior under out-of-plane shear. For combined loading of core compression and in-plane tension, the edges of the web aligned with the direction of loading are displaced relative to one another uniformly, while a uniform crushing displacement is imposed. The calculated initial yield surfaces for the aforementioned combinations of loading, along with the prediction from the ellipsoidal yield surface invoked in the proposed constitutive model when all the plastic Poisson ratios are zero, are presented in Figure 3. Note that in the proposed constitutive model, an ellipsoidal yield surface is invoked that generalizes Hill's surface for orthotropic plastically incompressible materials. This ellipsoidal yield surface can be written in the form of

$$f \equiv \sigma_{\text{eff}} - \sigma_0 = 0$$

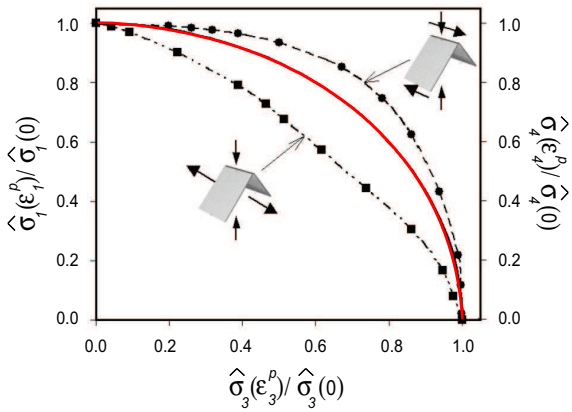

Figure 3. Initial yield surface of the folded plate core subject to two different combined loadings. The true stresses are normalized by the initial yield stress associated with each simple loading history under quasistatic loading. The solid line corresponds to the ellipsoidal yield surface invoked in the constitutive model when all the plastic Poisson ratios are taken to be zero. The folded core has the same geometrical parameter as that in Figure 2.

where the effective stress σ_{eff} is defined by

$$(\sigma_{\text{eff}}/\sigma_0)^2 = \sum_{i=1}^{6} (\sigma_i/\hat{\sigma}_i)^2$$

for the case that plastic Poisson ratios are zero. The stress quantity σ_0 is a fixed reference stress that can be chosen arbitrarily. $\hat{\sigma}_i(\varepsilon_i^P)$ denotes the hardening (or softening) function specifying the dependence of σ_i on the associated plastic strain component. See [Xue et al. 2005] for details. Figure 3 shows that the unit cell results for combination of crushing and out-of-plane shear indicate that the proposed constitutive model overestimates the interaction among the stresses under this loading condition at early stages of deformation. For combined core crushing and in-plane tension, the folded plate core has an initial yield surface which nearly mimics the generalized Hill's surface for orthotropic plastic incompressible materials, as the plastic incompressibility of the steel core contributes remarkably to its overall behavior at the onset of plastic deformation. As the deformation proceeds under combined core crushing and in-plane tension, the apparent plastic Poisson ratio abruptly decreases and then approaches zero, and the calculated yield surface approaches the prediction from the proposed constitutive model. This happens for an effective plastic strain smaller than 5%. (The numerical results are not shown for the sake of brevity).

Similar computations are performed for the folded plate core with higher core volume fraction $\bar{\rho}_c = 0.04$ ($\alpha = 45°$, $t/H = 0.0295$), for which the material yielding precedes the buckling of the core under core crushing. The computed initial yield surfaces associated with each loading combination are very close to the yield surface invoked in the proposed constitutive model. Similar conclusions are made for the response of the square honeycomb cores [Xue et al. 2005], hexagonal aluminum honeycomb with volume fraction of 0.02 [Doyoyo and Mohr 2003; Mohr and Doyoyo 2004] and pyramidal truss cores

(results not shown). The initial yield surface and failure surface of metal sandwich cores, specifically honeycomb cores under an in-plane state of stress, have been reported by several groups [Gibson et al. 1989; Papka and Kyriakides 1999; Okumura et al. 2002]. Wang and McDowell [2005] studied the initial yield surface of several periodic metal honeycomb cores with high relative density under in-plane biaxial and triaxial stress states. For all the cases studied, the relative density of the core is sufficiently high that the initial nonlinearity of the response is mainly due to plastic yielding of the core material. The developed analytical model revealed a strong interaction between stresses for combined loading of crushing and in-plane stretching.

3.2. ***Numerical results for unit cell response under dynamic loading.*** In this section, we study the rate-dependent behavior of the folded plate core under crushing and out-of-plane shear. The boundary conditions associated with each loading history are similar to those described in Section 3.1. Rigid plates are bonded to the top and bottom surfaces of the unit cell to simulate the behavior of the core attached to the face sheets. Equal and opposite constant velocities, V_3 and V_4, are applied to the top and bottom rigid faces to invoke a constant strain rate for core crushing and for shearing, respectively. The center of mass of the core is stationary during each loading. The associated overall strain rates of the core are defined as $\dot{\bar{\varepsilon}}_3 = 2V_3/H$ for dynamic core crushing and $\dot{\bar{\varepsilon}}_4 = 2V_4/H$ for dynamic core shearing.

The dependence of the overall crushing response of the folded core on the overall strain rate is presented in Figure 4a. The overall compressive stress, $\hat{\sigma}_3$, is normalized by its theoretical quasistatic initial yield value, $\hat{\sigma}_3(0)$ (from Equation (7)). The range of crushing strain rates selected in Figure 4a is widely representative of shock-loaded metal sandwich plates. The deformed configurations of the folded core subject to various crushing strain rates are depicted in Figure 4b at the overall crushing strain of 0.5, that is, the relative displacement of top and bottom faces is equal to half of the original core height. The strain rate dependence of core response is related to three effects: (i) inertia resistance in the vertical direction, (ii) inertial stabilization of the core plates against buckling, and (iii) contact between the core plates and top and bottom faces. Note that the material strain rate-dependence is not taken into account in these calculations. The inertia resistance elevates the level of stress at early stages of deformation. It is informative to compare these results with those of the square honeycomb core with the same steel core density presented in [Xue et al. 2005]. The influence of inertia resistance at early stages of deformation appears to be similar for both core topologies. However, while the core resistance can be maintained up to large deformations for the square honeycomb core, it falls steadily with deformation for the folded core as seen in Figure 4b. In general, the webs of the square honeycomb do not come in contact with the bottom and top faces except at very large core compressions, while the webs of the folded plate core make contact with the faces at relatively early stages of crushing. Increasing the strain rate alters the underlying mechanism of crushing deformation of the folded plate core; higher strain rates lead to a more localized deformation of the folded plate at the junctions with the face sheets resulting in earlier contact of the folded plate with the face sheets. The contacts elevate the overall crushing strength of the folded core at relatively early stages of deformation (for example, for $\dot{\bar{\varepsilon}}_3 = 2000\,\mathrm{s}^{-1}$ at the effective plastic strain $\sim$0.12). This phenomenon is to some extent analogous to the densification effect of the foam materials at high levels of deformation. As the deformation proceeds, a secondary elevation of stress is observed due to additional contacts, occurring at much larger deformations (for example, for $\dot{\bar{\varepsilon}}_3 = 2000\,\mathrm{s}^{-1}$ at the effective plastic strain $\sim$0.85, see inset of Figure 4a). Larger deformations result in the full densification

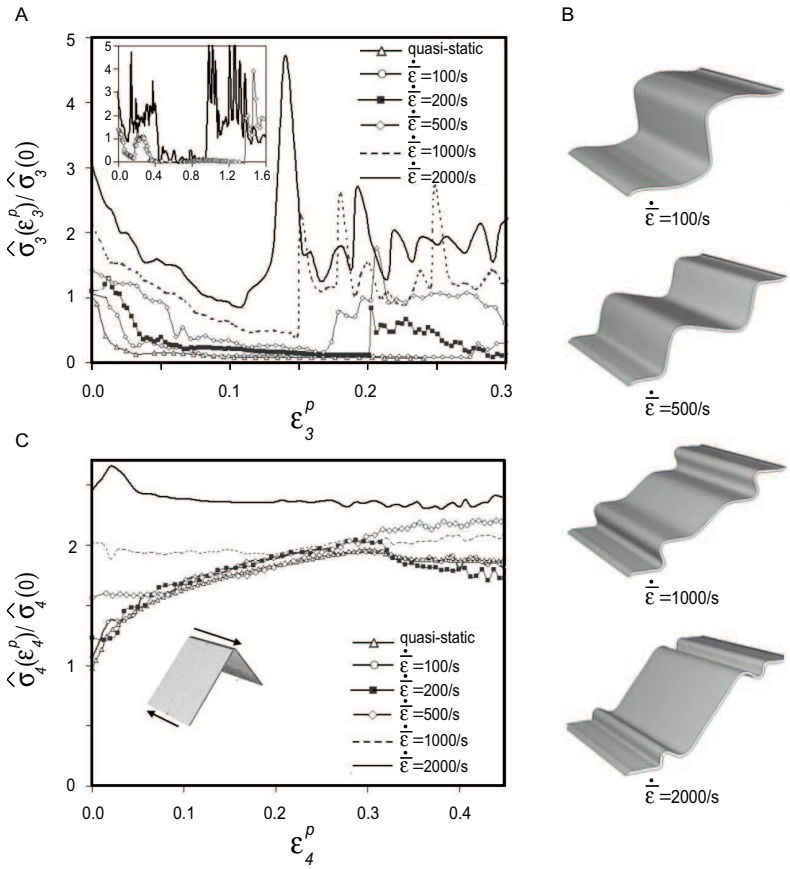

Figure 4. Rate dependence behavior of folded plate cores: (a) effect of crushing rate on the normalized true stress-true plastic strain relation of the folded core under core crushing. Inset: additional contacts occur at large deformations which lead to sudden elevation of stress; (b) deformed configurations of the folded plate core unit cell subject to various crushing rates at average crushing strain of 0.5; (c) dynamic response of the folded plate core under out-of-plane shear. The true stresses are normalized by the theoretical values of the initial yield stress associated with each loading history under quasistatic loading, Equation (7). The folded core has the same geometrical parameter as that in Figure 2.

of the core. It is noteworthy that at high strain rates, square honeycomb cores are more effective than folded plate cores for energy dissipation, mainly due to stabilization of the webs against buckling, an effect that promotes the axial compression of the webs. We will discuss this further when assessing the response of folded sandwich plates under high intensity loading in Section 5.2.

Figure 4c presents the overall out-of-plane shear response of the folded core (normalized by its theoretical quasistatic initial yield values, $\hat{\sigma}_4(0)$) subjected to various engineering strain rates. The strain rate-dependence of the dynamic core shearing is mainly attributed to the microinertia effects and stabilization

of the core plate against shear buckling. The contact between the core plate and face sheets is not evident in the range of deformation considered in Figure 4c.

4. Pyramidal truss core unit cell response

The geometry of the pyramidal truss core along with the coordinate system used to define the anisotropy are depicted in Figure 5a. In the computational model, the ends of the truss members are constrained, assuming that the ends are welded to the rigid face sheets. The overall elastic moduli associated with crushing and out-of-plane shear responses of the pyramidal truss core are estimated based on simple strength-of-materials formulas as follows:

$$\begin{aligned} E_{22} &= \bar{\rho}_c E \sin^4 \alpha, \\ G_{12} = G_{23} &= \frac{1}{8} \bar{\rho}_c E \sin^2 2\alpha. \end{aligned} \tag{8}$$

Estimates for the initial quasistatic yield values, $\hat{\sigma}_i(0)$, are given by,

$$\begin{aligned} \hat{\sigma}_3(0) &= \sigma_Y \bar{\rho}_c \sin^2 \alpha, \\ \hat{\sigma}_4(0) = \hat{\sigma}_5(0) &= \frac{1}{2\sqrt{2}} \sigma_Y \bar{\rho}_c \sin 2\alpha. \end{aligned} \tag{9}$$

The pyramidal truss core responses under quasistatic and dynamic loadings are calculated for the following geometrical parameters: $\alpha = 45^\circ$, $t/H = 0.1055$, which corresponds to $\bar{\rho}_c = 0.02$.

4.1. ***Numerical results for unit cell response under quasistatic loading.*** In this section are described simulations that have been performed to ascertain the basic stress histories of the pyramidal truss core under crushing and out-of-plane shear, Figure 5b. The imposed boundary conditions associated with each loading history are similar to those employed in Section 3.1 for the folded plate core. Under crushing, yielding of the truss members is followed by their plastic buckling, which results in a significant reduction in the load carrying capacity of the core under crushing. As in the case of folded plate cores, at large deformation the truss members make contact with the rigid face sheets. This contact leads to a significant elevation in the load carrying capacity of the pyramidal truss core, analogous to the effect of densification on the crushing response of foam materials. The displaced configurations of the pyramidal truss core at different overall crushing strains are depicted in Figure 5c. The overall response of the pyramidal truss core under out-of-plane shear is associated with utterly dissimilar deformations of the truss members: two of the truss members of the core unit cell shown in Figure 5a undergo stretching, while the other two truss members experience compression. As the deformation proceeds, the plastic yielding of the truss cores is followed by the buckling of the members under compression, which leads to a considerable reduction in the load carrying capacity of the pyramidal truss core, Figure 5b. The softening exhibited by the core under out-of-plane shear is contrary to the behavior of folded plate and square honeycomb cores where the webs undergo plastic buckling but with no significant softening. For sandwich plates with the overall geometry on the meter scale under quasistatic loading, the first occurrence of nonlinearity in most applications is related to buckling of core members due to out-of-plane shear as discussed for rigid punch indentation of folded sandwich plates in Section 5.1. The softening of the pyramidal truss core under out-of-plane shear could jeopardize the structural performance of pyramidal truss core sandwich

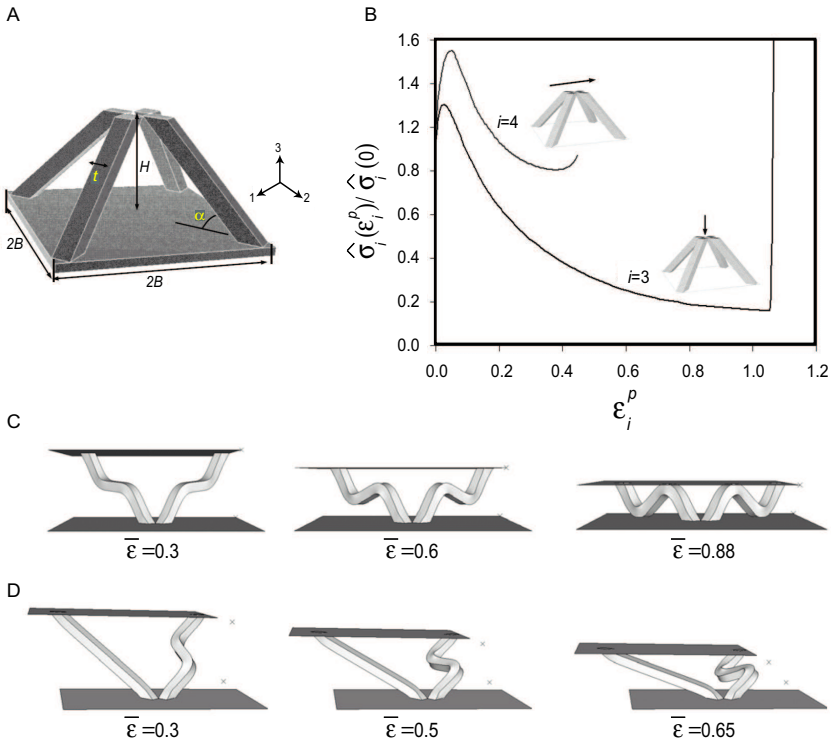

Figure 5. Mechanical behavior of pyramidal truss cores: (a) schematic diagram of a pyramidal truss core unit cell; (b) normalized true stress-true plastic strain response of the pyramidal truss cores with $\alpha = 45°$, $t/H = 0.1055$, corresponding to $\bar{\rho}_c = 0.02$ under two basic loading histories. The true stresses are normalized by the theoretical values of the initial yield stress associated with each loading history under quasistatic loading; see Equation (9) (c) and (d); deformed configurations of the pyramidal truss core unit cell at different levels of average engineering strain, $\bar{\varepsilon}$, subject to core crushing (c) and out-of-plane shear (d).

plates [Xue and Hutchinson 2004a]. Figure 5d depicts the displaced configurations of the pyramidal truss core at different overall shear strains. It is also noteworthy that the strength and stiffness associated with in-plane stretching and shearing are exceptionally low for pyramidal truss cores but of little consequence to the structural performance of the sandwich plates in most applications.

4.2. ***Numerical results for unit cell response under dynamic loading.*** Finite element simulations have been carried out to study the effect of deformation rate on the dynamic behavior of the pyramidal truss core under crushing and out-of-plane shear following the same procedure discussed in Section 3.2. The overall responses of the pyramidal truss core subject to different crushing strain rates are depicted in Figure 6a. Firstly, inertia resistance in the vertical direction, which manifests as plastic wave propagation, elevates the initial level of stress [Vaughn et al. 2005]. Secondly, the core starts to soften at very early stages of deformation due to the buckling of each truss member triggered by its tilt. Thirdly, the contact between the truss members and the faces generally does not occur until relatively large

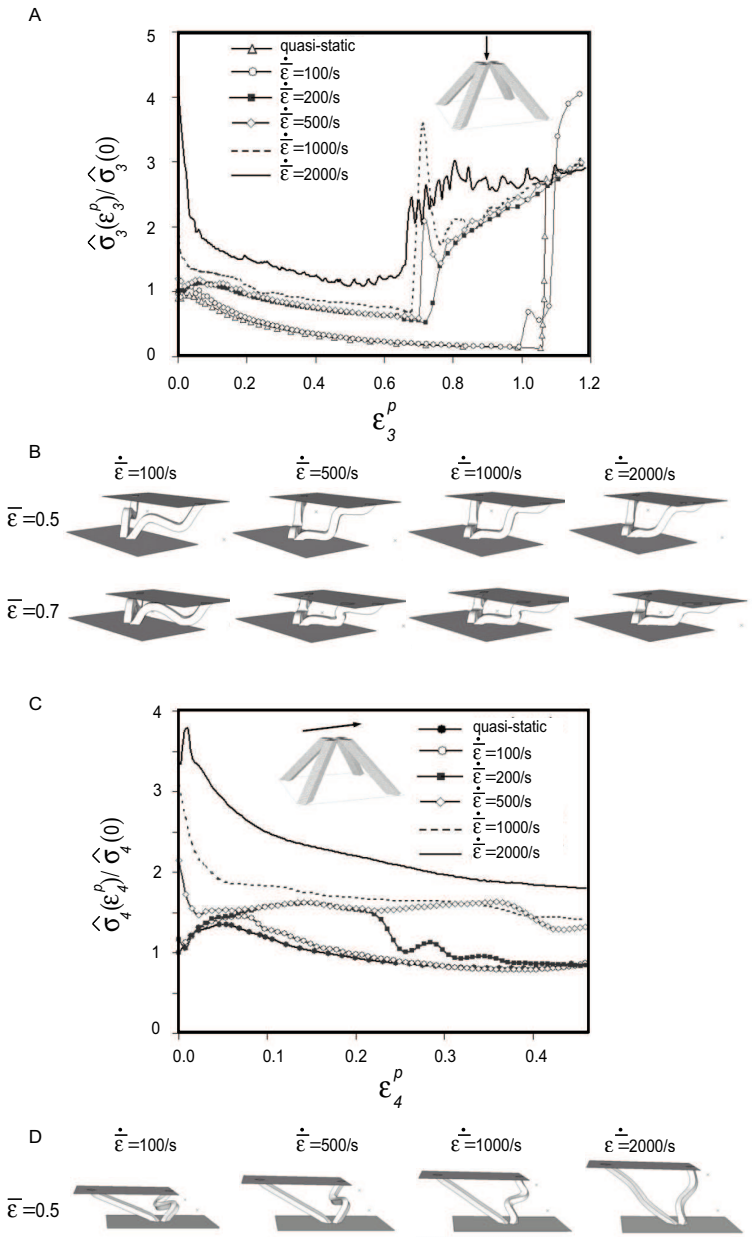

Figure 6. Rate dependence behavior of pyramidal truss cores. Dynamic response of a pyramidal truss core with $\alpha = 45°$, $t/H = 0.1055$, corresponding to $\bar{\rho}_c = 0.02$ under crushing and out-of-plane shear at different deformation rates is quantified in (a) and (c), respectively. Deformed configurations of the pyramidal truss core under crushing at different crushing rates are depicted in (b) at two different stages of deformation corresponding to average crushing strain of 0.5 and 0.7. Similarly, the deformed configurations of the core subject to out-of-plane shear at different strain rates are shown in (d) at the average crushing strain of 0.5. The pyramidal truss core has the same geometrical parameter as that in Figure 5.

deformations, which results in a sudden increase in the load carrying capacity of the core under crushing. It is noteworthy that there is little difference between deformed configurations of the truss cores subject to crushing strains in the range of 200–2000 s^{-1}, leading to low sensitivity for the onset of densification on the crushing strain rate (the contact between the truss cores and the face sheets occurs at the plastic strain of $\varepsilon_3^p \sim 0.7$ for overall strain rates equal to or higher than 200 s^{-1}). This is in sharp contrast to the response exhibited by the folded plate cores in Figure 4a and 4b, where the crushing rate significantly alters the deformation of the core.

The dynamic shear response of the pyramidal truss core is quantified in Figure 6c. The deformed configurations of the pyramidal truss core, subject to various strain rates under out-of-plane shear, are depicted in Figure 6d at an average crushing strain of 0.5. At high deformation rates, the inertia resistance enhances the overall dynamic strength of the pyramidal truss core by elevating the level of stress of the truss members under stretching, and also by stabilizing the members, which undergo shear-induced compaction. This leads to an utterly different overall behavior compared to folded plate cores (see Section 3.2) and square honeycomb cores [Xue et al. 2005].

5. Folded sandwich plate response

Computational tools are indispensable for augmenting experimental techniques for assessing the structural performance of metal sandwich plates. This, in general, entails full three-dimensional models of sandwich plates subject to quasistatic and dynamic loading, and consideration of the geometrical details of the core [Xue and Hutchinson 2004a]. These calculations are extremely expensive and even unrealistic for complex structures. Such computation limitations motivate an alternative approach based on continuum representation of the metal cores. Recently, we have developed a constitutive model for the elastic-plastic behavior of plastically compressible orthotropic materials with nonuniform hardening or softening evolution in different stressing directions. This constitutive model invokes an ellipsoidal yield surface with evolving ellipticity to accommodate the nonuniform stress-strain responses under the six fundamental stress histories in the orthotropic axes. Furthermore, the model is able to incorporate rate-dependence arising from material rate-dependence, inertial effects, as well as geometrical constraints (for example, contact). The general formulation of the constitutive model for plastically compressible orthotropic materials is able to incorporate nonconstant plastic Poisson ratios in the axes of anisotropy (for example, the plastic Poisson ratios can be a function of plastic strain). However, for the sandwich plates under study, the plastic deformation of the core is well approximated by taking all plastic Poisson ratios as zero. The readers are referred to [Xue et al. 2005] for details of the constitutive model. The proposed model is employed in this paper to investigate the structural role of sandwich cores on the overall response of folded sandwich plates, and complements our previous work on the structural performance of square honeycomb sandwich plates [Xue et al. 2005]. Specifically, infinite folded plates of width 2m that are clamped along their edges (Figure 1) and subject to (i) quasistatic punch load and (ii) dynamic impulsive pressure load, are considered to illustrate the applicability of the proposed constitutive model for simulating and predicting the overall response of sandwich plates. To assess the accuracy of the approach based on the constitutive model, a set of calculations is performed using three-dimensional finite element models of the folded core with full meshing of the core geometrical details. Three-dimensional finite element models employ the geometrical unit of the plate, exploiting the

periodicity of the plate in its long direction. The faces are modeled by the classical plasticity with the von Mises yield criterion and isotropic hardening, with material properties given in Section 2. On the other hand, finite element models of the sandwich plate with continuum core models satisfy plane strain conditions for the loadings under study in this section, rendering the problem two dimensional. In all the calculations, which employ the proposed core continuum model, the core is modeled using one element through thickness. It is noteworthy that the proposed core continuum model, as a macroscopic modeling approach, cannot predict the details of structural localization. This is discussed further in [Mohr et al. 2006].

5.1. ***Numerical results for quasistatic loading of folded sandwich plate.*** Like the plate, the rigid punch in Figure 7a is infinite in the direction perpendicular to the cross-section shown, and has the half-width and edge radius of $a_{\text{punch}}/L = 0.3$ and $R_{\text{punch}}/a_{\text{punch}} = 0.334$, respectively. The sandwich plate has the normalized mass per unit area, $M/(\rho_s L) = 0.02$. For clamped sandwich plates subject to transverse loads, the important basic stressing histories of the core are: crushing normal to the sandwich faces; out-of-plane shear; and in-plane stretching. Here, the flexibility offered by the core constitutive model is employed to highlight the role of individual basic stressing histories of the core on the overall performance of sandwich plates. Calculations for three sets of inputs have been carried out:

(A) All six input functions, $\hat{\sigma}_i$. The stress-strain response under each basic stressing history is transferred directly from the numerical simulations presented in Section 3.1 into the code.

(B) Uniform hardening with all components specified by the crushing response, $\hat{\sigma}_i = \hat{\sigma}_3$

(C) Uniform hardening with all components specified by the shear response, $\hat{\sigma}_i = \hat{\sigma}_4$.

For each set of calculations, the elastic constants and the initial yields are predicted based on simple strength-of-material relations, Equations (5), and (7). The constitutive model provides two hardening formulations for representing the core behavior as outlined in [Xue et al. 2005]. In this paper, all the calculations are performed using the Coupled Hardening Formulations.

Figure 7b displays the variation of normalized reacting force/length of the punch, P/P_c versus the normalized displacement of the punch, δ_{Punch}/L based on the full three-dimensional simulation and also the continuum models with the abovementioned inputs (A–C). P_c is the limit load/length for a perfectly plastic empty sandwich plate having limited bending moment/length, (based only on contributions from the faces), for example,

$$P_c = 4\sigma_Y h H/L. \tag{10}$$

The variation of the average compressive strain of the folded plate core at its middle section,

$$\bar{\varepsilon}_c = \Delta H/H$$

(where ΔH is the reduction in core height), with the normalized punch displacement, δ_{Punch}/L, for the same set of simulations is depicted in Figure 7c. The dimensions of the sandwich plate and its material properties are such that the core yielding in shear is the first occurrence of nonlinear behavior followed by core crushing due to elastic buckling of the core plate beneath the punch. The same mechanism of response is observed for square honeycomb and pyramidal truss sandwich plates with the same steel core density. However, the elastic buckling of the square honeycomb cores occurs at significantly larger punch displacement. The results from the three-dimensional finite element simulation indicate that the

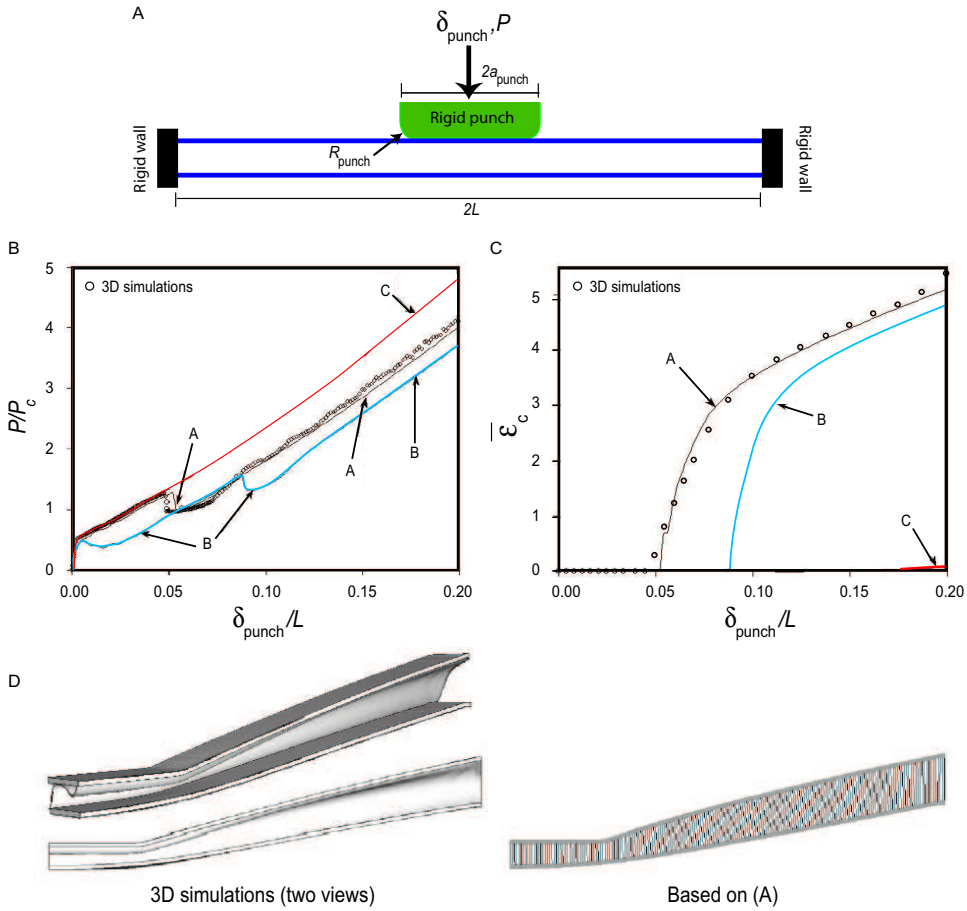

Figure 7. Folded sandwich plates subject to quasistatic rigid punch indentation: (a) schematic diagram of the folded core sandwich plate subject to punch loading; the rigid punch is infinite in the direction perpendicular to the cross-section shown and has normalized half width of $a_{\text{punch}}/L = 0.3$ and normalized edge radius of $R_{\text{punch}}/a_{\text{punch}} = 0.334$. The folded core has the same geometrical parameter as that in Figure 2. The sandwich plate has the total mass per unit area, $M/(\rho_s L) = 0.02$; (b) normalized reaction force applied to the rigid punch, P/P_c verses normalized punch displacement, δ_{Punch}/L, obtained based on both the three-dimensional finite element model of the sandwich plate and the proposed continuum core model; (c) dependence of the average compressive strain of the core at its center, $\bar{\varepsilon}_c$, on the normalized punch displacement, δ_{Punch}/L; (d) deformed configuration at $\delta_{\text{Punch}}/L = 0.2$ predicted from the three-dimensional finite element model and by employing input set A in the proposed continuum core model.

elastic buckling of the core occurs at $\delta_{\text{Punch}}/L \approx 0.05$. By employing the input set (C), the initial nonlinear response of the sandwich plate can be predicted accurately. However, the unrealistic hardening behavior in crushing represented by (C), as opposed to softening, suppresses nearly all core crushing, as is evident in Figures 7c and 7d. On the other hand, uniform *hardening* based on inputting the crushing

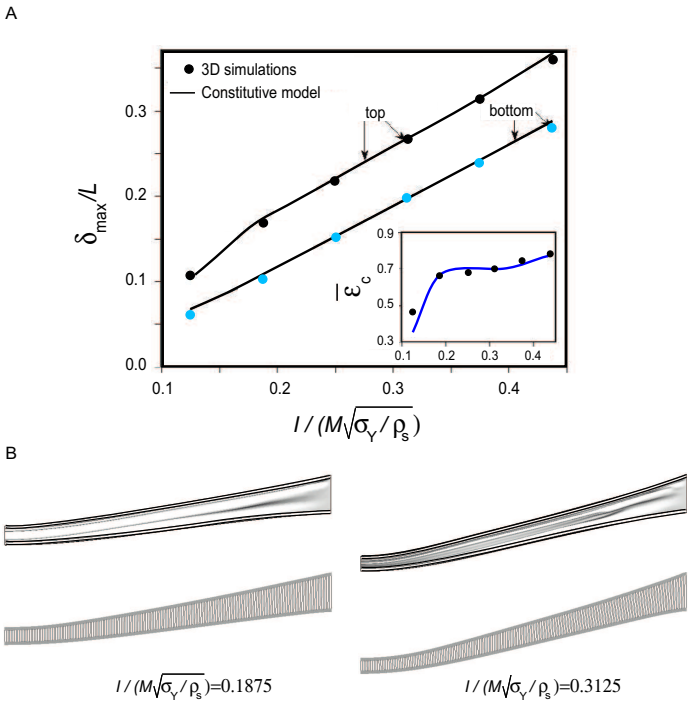

Figure 8. Folded sandwich plates subject to uniform shock loading: (a) normalized maximum deflection of the top and bottom faces of the folded sandwich plate versus normalized momentum imparted to the sandwich plate, $I/(M\sqrt{\sigma_Y/\rho_s})$. Inset: Residual average compressive strain of the core at its middle, $\bar{\varepsilon}_c$, versus $I/(M\sqrt{\sigma_Y/\rho_s})$. The results are obtained based on both three-dimensional finite element model of the sandwich plate and the proposed continuum core model. The sandwich plate has the same geometrical parameter as that in Figure 7. (b) Finalized deformed configurations of the folded core sandwich plates subject to two different impulse levels predicted using the three-dimensional finite element model (left) and the proposed continuum core model (right).

stress-strain curve (B) severely underestimates the early strength of the sandwich plate because of the unrealistic representation of the shear behavior. The inputs using all six basic stress-strain curves (A) rather accurately reproduce the entire load-deflection curve, as well as the crushing strain. The displaced configuration of the folded sandwich plates corresponding to $\delta_{\text{Punch}}/L = 0.2$ under the rigid indentation load applied at the center of the sandwich plate for the three dimensional finite element model and also the model based on the continuum representation of the core based on (A) are depicted in Figure 7d.

5.2. ***Numerical results for dynamic loading of folded sandwich plate.*** For $t \geq 0$, a pressure $p = p_0 e^{-t/t_0}$ is applied uniformly over the upper face sheet of the sandwich plate to simulate a shock transmitted through air to the metal sandwich plates [Taylor 1963; Smith and Hetherington 1994]. The decay time of the pressure pulse is set at $t_0 = 10^{-4}$ s, which is a typical decay period for a high intensity pulse

generated in air. Without accounting for fluid-structure interaction, the transmitted momentum/area is $I_0 = \int_0^\infty p dt = p_0 t_0$.

Computations are carried out at different levels of dynamic loading as measured by the normalized impulse $I/(M\sqrt{\sigma_Y/\rho_s})$. The inputs to the constitutive model are identified using the numerical simulations presented in Section 3. Figure 8a presents the normalized maximum deflection of the top and bottom faces, $\delta_{\max}/L$, and the crushing strain in the center of the plate at the final deformed state as a function of the dimensionless impulse. For the folded sandwich plate under study, the excessive crushing of the steel core clearly compromises the performance of the sandwich plate such that the crushing strain is almost 75%. Figure 8b compares the final deformed state predicted by the three-dimensional finite element simulations with that based on the constitutive model for two different levels of impulse. It is clear from Figure 8 that the continuum constitutive model captures the overall deflection of the sandwich plate, as well as the average crushing strain of the folded plate core with remarkable fidelity.

An additional set of calculations is carried out to highlight the effect of rate-dependent behavior of the core under crushing on the overall response of the folded sandwich plate. The calculations are performed by employing the constitutive model without accounting for the strain rate influence when representing the core behavior under crushing (for example, a quasistatic response is used to represent the core response under crushing). Although there are some differences in the details of the response, such as the history of energy dissipation in the sandwich plate constituent, the finalized configurations and the overall performance of the folded sandwich plate can be predicted accurately using this model. The behavior of folded sandwich plates is different from that of the square honeycomb sandwich plates in which case ignoring the dependence of the crushing response on the deformation rate significantly underestimates their structural performance under a high intensity pulse [Xue et al. 2005]. As discussed in Section 3.2, the plastic energy dissipation associated with core crushing is not significantly altered by varying the strain rates for folded plate cores. It is also noteworthy that in most applications, the core shearing strain rate in metal sandwich plates is considerably lower than $1000\,\mathrm{s}^{-1}$. In this range, the rate-dependent behavior of a metal core subject to out-of-plane shear is not significant and can be neglected in analyzing the structural performance of sandwich plates.

6. Concluding remarks

Metal sandwich plates have been considered recently for designing high-performance structures, specifically for enhancing the resistance of structures under shock loading. The structural performance of metal sandwich plates under dynamic loading, which involves both material and geometric nonlinearity, is governed by complex localized phenomena, including dynamic buckling and microinertial resistance associated with core crushing. In the present study, mechanical behavior of folded plate and pyramidal truss metal cores under both quasistatic and dynamic loadings are discussed. This study complements previous studies on the mechanical behavior of square honeycomb cores [Xue et al. 2005; Xue and Hutchinson 2006], pyramidal truss cores [Lee et al. 2006] and polymeric foam-filled cores [Vaziri et al. 2006], and has direct implications in designing high-performance metal sandwich plates. This study also further emphasizes the importance of 'core topology' as one of the major design criteria for metal sandwich plates, as also illustrated in studies on failure of metal sandwich plates [Vaziri et al. 2007]. In the second part of this study, a recently-developed constitutive model for the elastic-plastic behavior

of orthotropic materials with nonuniform hardening or softening under stressing in different directions [Xue et al. 2005] is employed to study the structural response of large scale folded metal sandwich plates under both quasistatic and dynamic loadings. Insights into the structural performance of these structures, specifically the role of core material behavior, are gained by using the capabilities of the proposed constitutive model such as selecting the input curves which represent the rate-dependent behavior of the core material under each basic stressing history.

Acknowledgment

The authors thank Prof. John W. Hutchinson for many insightful discussions. Correspondence and requests for materials should be addressed to A. V.

References

[Abaqus 2005] Abaqus, *Abaqus version 6.5 reference manuals*, Abaqus Inc., Providence, R.I., 2005.

[Boyer and Gall 1985] H. E. Boyer and T. L. Gall, *Metals handbook desk edition*, American Society for Metals, 1985.

[Doyoyo and Mohr 2003] M. Doyoyo and D. Mohr, "Microstructural response of aluminum honeycomb to combined out of plan loading", *Mech. Mater.* **35** (2003), 865–876.

[Fleck and Deshpande 2004] N. A. Fleck and V. S. Deshpande, "The resistance of clamped sandwich beams to shock loading", *J. Appl. Mech. (Trans. ASME)* **71** (2004), 386–401.

[Gibson et al. 1989] L. J. Gibson, M. F. Ashby, J. Zhang, and T. C. Triantafillou, "Failure surfaces for cellular materials under multiaxial loads I. Modeling", *Int. J. Mech. Sci.* **31** (1989), 635–663.

[Hutchinson and Xue 2005] J. W. Hutchinson and Z. Xue, "Metal sandwich plates optimized for pressure impulses", *Int. J. Mech. Sci.* **47** (2005), 545–569.

[Lee et al. 2006] S. Lee, F. Barthelat, J. W. Hutchinson, and H. D. Espinosa, "Dynamic failure of metallic pyramidal truss core materials - Experiments and modeling", *Int. J. Plasticity* **22** (2006), 2118–2145.

[Liang et al. 2007] Y. Liang, A. V. Spuskanyuk, S. E. Flores, D. R. Hayhurst, J. W. Hutchinson, R. M. McMeeking, and A. G. Evans, "The response of metallic sandwich panels to water blast", *J. Appl. Mech. (Trans. ASME)* **74** (2007), 81–99.

[Mohr and Doyoyo 2004] D. Mohr and M. Doyoyo, "Experimental investigation on the plasticity of hexagonal aluminum honeycomb under multiaxial loading", *J. Appl. Mech. (Trans. ASME)* **71** (2004), 375–385.

[Mohr et al. 2006] D. Mohr, X. Z., and A. Vaziri, "Quasi-static punch indentation of a honeycomb sandwich plate: Experiments and modeling", *J. Mech. Mater. Struct.* **1**:3 (2006), 581–604.

[Okumura et al. 2002] D. Okumura, N. Ohno, and H. Noguchi, "Post-buckling analysis of elastic honeycombs subject to in-plane biaxial compression", *Internat. J. Solids Structures* **39** (2002), 3487–3503.

[Papka and Kyriakides 1999] S. D. Papka and S. Kyriakides, "Biaxial crushing of honeycombs-Part 1: Experiments", *Internat. J. Solids Structures* **36** (1999), 4367–4396.

[Qiu et al. 2003] X. Qiu, V. S. Deshpande, and N. A. Fleck, "Finite element analysis of the dynamic response of clamped sandwich beams subject to shock loading", *Eur. J. Mech. A: Solids* **22** (2003), 801.

[Rathbun et al. 2006] H. J. Rathbun, D. D. Radford, Z. Xue, M. Y. He, J. Yang, V. Deshpande, N. A. Fleck, J. W. Hutchinson, F. W. Zok, and A. G. Evans, "Performance of metallic honeycomb-core sandwich beams under shock loading", *Internat. J. Solids Structures* **43** (2006), 1746–1763.

[Smith and Hetherington 1994] P. D. Smith and J. G. Hetherington, *Blast and ballistic loading of structures*, Butterworth-Heinemann, Oxford, 1994.

[Taylor 1963] G. I. Taylor, "The pressure and impulse of submarine explosion waves on plates", pp. 287–303 in *The scientific papers of sir Geoffrey Ingram Taylor, volume III: Aerodynamics and the mechanics of projectiles and explosions*, edited by G. K. Batchelor, Cambridge University Press, 1963.

[Vaughn et al. 2005] D. Vaughn, M. Canning, and J. W. Hutchinson, "Coupled plastic wave propagation and column buckling", *J. Appl. Mech. (Trans. ASME)* **72** (2005), 1–8.

[Vaziri and Hutchinson 2007] A. Vaziri and J. W. Hutchinson, "Metal sandwich plates subject to intense air shocks", *Internat. J. Solids Structures* **44** (2007), 2021–2035.

[Vaziri et al. 2006] A. Vaziri, Z. Xue, and J. W. Hutchinson, "Metal sandwich plates with polymeric foam-filled cores", *J. Mech. Mater. Struct.* **1** (2006), 95–128.

[Vaziri et al. 2007] A. Vaziri, Z. Xue, and J. W. Hutchinson, "Performance and failure of metal sandwich plates subject to shock loading", *J. Mech. Mater. Struct.* (2007). in press.

[Wang and McDowell 2005] A. J. Wang and D. L. McDowell, "Yield surfaces of various periodic metal honeycombs at intermediate relative density", *Int. J. Plasticity* **21** (2005), 285–320.

[Xue and Hutchinson 2003] Z. Xue and J. W. Hutchinson, "Preliminary assessment of sandwich plates subject to blast loads", *Int. J. Mech. Sci.* **45** (2003), 687–705.

[Xue and Hutchinson 2004a] Z. Xue and J. W. Hutchinson, "A comparative study of impulse-resistant metallic sandwich plates", *Int. J. Impact Engineering* **30** (2004a), 1283–1305.

[Xue and Hutchinson 2004b] Z. Xue and J. W. Hutchinson, "Constitutive model for quasi-static deformation of metallic sandwich cores", *Internat. J. Numer. Methods Engrg.* **61** (2004b), 2205–2238.

[Xue and Hutchinson 2006] Z. Xue and J. W. Hutchinson, "Crush dynamics of square honeycomb sandwich cores", *Internat. J. Numer. Methods Engrg.* **65** (2006), 2221–2245.

[Xue et al. 2005] Z. Xue, A. Vaziri, and J. W. Hutchinson, "Non-uniform constitutive model for compressible orthotropic materials with application to sandwich plate cores", *Computer Modeling in Engineering and Applied Sciences* **10** (2005), 79–95.

Received 17 Apr 2007. Accepted 17 Apr 2007.

ASHKAN VAZIRI: avaziri@seas.harvard.edu
School of Engineering and Applied Sciences, Harvard University, Cambridge, MA 02138, United States
www.seas.harvard.edu/~avaziri

ZHENYU XUE: xue@seas.harvard.edu
School of Engineering and Applied Sciences, Harvard University, Cambridge, MA 02138, United States